ORIGINAL RESEARCH ARTICLE

PHARMACOLOGICAL STRATEGIES IN LUNG CANCER-INDUCED CACHEXIA: EFFECTS ON MUSCLE PROTEOLYSIS, AUTOPHAGY, STRUCTURE, AND WEAKNESS[†]

Alba Chacon-Cabrera[1,2], Clara Fermoselle[1,2], Alejandro J. Urtreger[3], Mercè Mateu-Jimenez[1,2], Miriam J. Diament[3], Elisa D. Bal de Kier Joffé[3], Marco Sandri[4], Esther Barreiro[1,2]

[1]Pulmonology-Lung Cancer Research Group, IMIM-*Hospital del Mar*, *Parc de Salut Mar*, Health and Experimental Sciences Department (CEXS), *Universitat Pompeu Fabra* (UPF), Parc de Recerca Biomèdica de Barcelona (PRBB), Barcelona, Spain.

[2]*Centro de Investigación en Red de Enfermedades Respiratorias* (CIBERES), *Instituto de Salud Carlos* III (ISCIII), Bunyola, Majorca, Balearic Islands, Spain.

[3]Research Area, Institute of Oncology 'Angel H. Roffo', University of Buenos Aires, Buenos Aires, Argentina.

[4]Department of Biomedical Sciences, University of Padova, Dubelcco Telethon Institute, Venetian Institute of Molecular Medicine, Padova, Italy.

Corresponding author: Dr. Esther Barreiro, Pulmonology Department-URMAR, IMIM-Hospital del Mar, PRBB, C/ Dr. Aiguader, 88, Barcelona, E-08003 Spain, Telephone: (+34) 93 316 0385, Fax: (+34) 93 316 0410, e-mail: ebarreiro@imim.es

Running head: muscle biology, structure, and function in cachexia

[†] This article has been accepted for publication and undergone full peer review but has not been through the copyediting, typesetting, pagination and proofreading process, which may lead to differences between this version and the Version of Record. Please cite this article as doi: [10.1002/jcp.24611]

Additional Supporting Information may be found in the online version of this article.

Abstract

Cachexia is a relevant comorbid condition of chronic diseases including cancer. Inflammation, oxidative stress, autophagy, ubiquitin-proteasome system, nuclear factor (NF)-κB, and mitogen activated protein kinases (MAPK) are involved in the pathophysiology of cancer cachexia. Currently available treatment is limited and data demonstrating effectiveness in *in vivo* models are lacking. Our objectives were to explore in respiratory and limb muscles of lung cancer (LC) cachectic mice whether proteasome, NF-κB, and MAPK inhibitors improve muscle mass and function loss through several molecular mechanisms. Body and muscle weights, limb muscle force, protein degradation and the ubiquitin-proteasome system, signaling pathways, oxidative stress and inflammation, autophagy, contractile and functional proteins, myostatin and myogenin, and muscle structure were evaluated in the diaphragm and gastrocnemius of LC (LP07 adenocarcinoma) bearing cachectic mice (BALB/c), with and without concomitant treatment with NF-κB (sulfasalazine), MAPK (U0126), and proteasome (bortezomib) inhibitors. Compared to control animals, in both respiratory and limb muscles of LC cachectic mice: muscle proteolysis, ubiquitinated proteins, autophagy, myostatin, protein oxidation, FoxO-1, NF-κB and MAPK signaling pathways, and muscle abnormalities were increased, while myosin, creatine kinase, myogenin, and slow- and fast-twitch muscle fiber size were decreased. Pharmacological inhibition of NF-κB and MAPK, but not the proteasome system, induced in cancer cachectic animals, a substantial restoration of muscle mass and force through a decrease in muscle protein oxidation and catabolism, myostatin, and autophagy, together with a greater content of myogenin, and contractile and functional proteins. Attenuation of MAPK and NF-κB signaling pathway effects on muscles is beneficial in cancer-induced cachexia.

Key words:

● **cancer-induced cachexia**

● **skeletal muscles**

2

● **proteolysis**

● **autophagy**

● **oxidative stress and inflammation**

● **muscle structure and function**

● **proteasome, NF-κB, and MAPK inhibitors**

INTRODUCTION

Muscle wasting and cachexia are important systemic manifestations of highly prevalent conditions including cancer. The prevalence of cachexia varies across diseases, but in advanced malignancies it ranges from 60 to 80% (von and Anker, 2010), being greater in patients with lung and gastrointestinal tumors than in other solid or hematologic malignancies (Muscaritoli et al, 2006). Cachexia, characterized by muscle mass loss and body composition alterations, has a negative impact on the patients' quality of life (Evans et al, 2008).

Although the etiology of cancer-induced cachexia remains to be fully understood, several cellular and molecular mechanisms have been proposed such as systemic inflammation(Argiles et al, 2011), oxidative stress (Barreiro et al, 2005;Barreiro et al, 2009;Marin-Corral et al, 2010;Mastrocola et al, 2008), metabolic disturbances and nutritional abnormalities(Barreiro et al, 2005;Barreiro et al, 2009;Morley et al, 2010). The myostatin and activin IIB system is also a relevant proposed mechanism contributing to muscle protein catabolism. Indeed, it was clearly demonstrated that the soluble receptor antagonist of myostatin (sActRIIB) improved muscle mass loss, survival and physical activity in cancer cachectic rodents (Busquets et al, 2012;Zhou et al, 2010). Furthermore, mitogen-activated protein kinases (MAPK) and nuclear factor (NF)-κB, which are central regulators of gene expression, redox balance, and metabolism, have also been shown to play a major role in adaptive or maladaptive responses to cellular stress within skeletal muscles (Kramer and

Goodyear, 2007). MAPK activation also seems to mediate oxidative stress-induced muscle atrophy (McClung et al, 2010). Interestingly, MAPK signaling was also shown to be involved in enhanced expression of proteasome via proteolysis-inducing factor in C_2C_{12} myotubes (Smith and Tisdale, 2003). However, studies demonstrating the potential beneficial effects of MAPK inhibition in cancer-induced cachexia *in vivo* are lacking.

NF-κB was also demonstrated to participate in the process of muscle wasting under several conditions such as sepsis (Penner et al, 2001), cancer cachexia (Cai et al, 2004;Moore-Carrasco et al, 2007), and chronic obstructive pulmonary disease (COPD) (Agusti et al, 2004;Moore-Carrasco et al, 2007). In fact, the double NF-κB and AP-1 inhibitor SP100030 elicited an improvement in muscle weights and markers of the ubiquitin-proteasome system (Moore-Carrasco et al, 2007). Sulfasalazine, a well-known drug used for the treatment of patients with inflammatory bowel disease and rheumatoid arthritis, is a potent and specific inhibitor of NF-κB. It inhibits its translocation into the nucleus, without affecting the activation of the AP-1 transcription factor (Wahl et al, 1998). Furthermore, that inhibition is accompanied by a blockade of the degradation of its inhibitory subunit IκB(Wahl et al, 1998). Sulfasalazine was also shown to restore tissue injury and function in several experimental models (Camara-Lemarroy et al, 2009;Olmez et al, 2008). However, the potential beneficial effects of NF-κB inhibition using sulfasalazine on cancer-induced cachexia are still unknown.

The ubiquitin-proteasome system plays a major role in conditions characterized by muscle wasting and weakness (Argiles and Lopez-Soriano, 1996;Fermoselle et al, 2011;Fermoselle et al, 2012;Olmez et al, 2008;Roth et al, 2005;van Hees et al, 2008;van et al, 2011). Specifically, bortezomib, the first proteasome inhibitor approved for use in patients, was demonstrated to significantly restore diaphragm muscle contractile function and myosin heavy chain content (MyHC) following coronary heart failure (van Hees et al, 2008) and elastase-induced emphysema(van et al, 2011). In another investigation (Supinski et al, 2009), however, bortezomib failed to improve the endotoxin-induced diaphragm dysfunction, while

partially restoring enhanced protein catabolism. Whether inhibition of the proteasome restores muscle mass and function in cancer cachexia remains to be identified.

As treatment options for cachexia are extremely limited and *in vivo* studies demonstrating the effectiveness of several potential anti-cachectic agents are clearly lacking, the current investigation was specifically designed to explore whether inhibitors of relevant cellular pathways such as MAPK, NF-κB, and the proteasome exert beneficial therapeutic effects on muscle mass loss and force generation in an in vivo experimental model of lung cancer cachexia in mice. Moreover, research conducted so far has mostly focused on the evaluation of limb muscles. On this basis, our objectives were to assess in respiratory and limb muscles from lung cancer (LC) cachectic mice receiving concomitant treatment with either MAPK, NF-κB, or proteasome inhibitors: 1) body and muscle weights, 2) limb muscle force, 3) proteolysis markers, 4) signaling pathways, 5) oxidative stress (protein carbonylation and nitration and antioxidant enzymes) and proinflammatory cytokines such as tumor necrosis factor (TNF)-alpha, interferon-gamma, interleukin (IL)-1beta and IL-6, 6) autophagy, 7) contractile and functional proteins, 8) myostatin and myogenin levels, and 9) muscle structural alterations.

MATERIALS AND METHODS

(See the supplementary online material for additional information on all methodologies).

Animal experiments

Tumor. LP07 cell line, which was previously obtained *in vitro* after successive passages of a P07 primary culture (Urtreger et al, 2001), derives from the transplantable P07 lung tumor that appeared spontaneously in the lung of a BALB/c mouse(Diament et al, 1998). LP07 cell line shares identical characteristics regarding lung tumor incidence and histology, and cachexia with its parental P07 tumor(Diament et al, 1998;Diament et al, 2006;Urtreger et al, 2001). Female BALB/c mice, 2 months old (weight ~20g), were obtained from Harlan

5

Interfauna Ibérica SL (Barcelona, Spain).

Experimental design. In all experimental groups (except for control rodents), LP07 viable cells ($4 \cdot 10^5$) resuspended in 0.2 mL minimal essential media (MEM) were subcutaneously inoculated in the left flank of the mice (day 1). All groups (n=10/group) were studied for a period of one month. Animals were randomly assigned to the following groups: 1) control, inoculation of 0.2 mL MEM in the left flank; 2) LC cachexia group, inoculation of LP07 cells; 3) LC cachectic mice received concomitant treatment with the proteasome inhibitor Bortezomib (Velcade, Millenium Pharmaceuticals, Cambridge, MA), 0.15 mg/Kg, 0.1 mL/6 days, intravenous injection into the tail vein (LC cachectic-bortezomib group) (Lu et al, 2006); 4) LC cachectic mice received concomitant treatment with sulfasalazine (Pfizer, Madrid, Spain), 200 mg/Kg, 0.3 mL/48h, intraperitoneal injection (LC cachectic-NF-κB inhibitor group) (Olmez et al, 2008); and 5) LC cachectic mice received concomitant treatment with the MAPK inhibitor U0126 (a highly selective inhibitor of MAP/ERK kinase (MEK)1/2 proteins, Selleck chemicals, Houston, TX), 30 mg/Kg, 0.1 mL/48h, intraperitoneal injection (LC cachectic-MAPK inhibitor group) (Schuh and Pahl, 2009). For ethical reasons, all pharmacological therapies were administered on day 15 after the inoculation of the LP07 cells up until the end of the study period (day 30). In order to assess the level of NF-κB transcription and *ex-vivo* protein degradation using the luciferase reporter and the tyrosine release assays, respectively (see below), a second batch of mice experiments was also conducted on identical experimental groups (N=10/group). One hind-limb and half of the diaphragm were used for each type of these experiments.

Ethics. All animal experiments were conducted in the animal facilities at *Parc de Recerca Biomèdica de Barcelona* (PRBB, Spain). This controlled study was designed in accordance with both the ethical standards on animal experimentation (EU 609/86 CEE, *Real Decreto* 1201/05 BOE 252, Spain) at PRBB and the European Convention for the Protection of Vertebrate Animals Used for Experimental and Other Scientific Purposes (1986). Ethical

6

approval was obtained by the Animal Research Committee at the Catalan Government (Animal welfare department, EBP-09-1228).

In vivo measurements and sample collection from mice

Body weight and food intake were determined every day during the entire duration of the study. Food and water were supplied ad libitum for the entire duration of the study protocol in the tumor-bearing mice. Control animals were paired-fed according to the amount of food eaten by the cachectic rodents. Limb strength was determined on days 0 and 30 using a strength grip meter (Bioseb, Chaville, France) following previously published methodologies, in which grip strength was also the end-point parameter in several experimental models of cancer cachexia in mice (Barreiro et al, 2010a;Murphy et al, 2012;Toledo et al, 2011;Vignaud et al, 2010;Whittemore et al, 2003). In the LC cachexia group of mice, tumor progression was determined using positron emission tomography (PET) (Figure E1) on days 13 and 20. Mice from all the experimental groups were always sacrificed on day 30 post-inoculation of LP07 cells or MEM (control animals). Each mouse was inoculated intraperitoneally with 0.1 mL sodium pentobarbital (60 mg/Kg). Diaphragm and gastrocnemius muscles and the subcutaneous tumor were obtained from all animals (Figure E2). The weight of both muscles and tumor was determined in each animal using a high-precision scale. Frozen tissues were used for immunoblotting and enzyme-linked immunosorbent assay (ELISA) techniques, while paraffin-embedded tissues were used for the assessment of muscle structure abnormalities and fiber type morphometry.

Muscle biology analyses

All muscle biology analyses were conducted blind in the same laboratory by the same investigators, at *Hospital del Mar*-IMIM (Barcelona).

Immunoblotting of 1D electrophoresis. Protein levels of the different molecular markers analyzed in the study were explored by means of immunoblotting procedures as previously described (Barreiro et al, 2010b;Barreiro et al, 2012;Fermoselle et al, 2011;Fermoselle et al,

2012;Marin-Corral et al, 2010). Protein content of markers of proteolysis, signaling pathways of muscle atrophy, redox balance, and different muscle proteins were identified using specific primary antibodies (See detailed information in the online supplementary material).

Protein catabolism. Protein degradation was explored on the basis of the rate of production of free tyrosine from tissue proteins as previously described (Tischler et al, 1982). As muscles cannot synthesize or degrade this amino acid, its accumulation reflects the net degradation of proteins. The results were expressed as nmol of tyrosine/mg of muscle/2 hours of incubation.

Luciferase reporter gene assay. On day 23 of the animal protocol (7 days exactly before sacrifice) all mice were injected in the right gastrocnemius muscle (for obvious reasons the diaphragm was not used for this purpose) with a mixture of 15 µg of control plasmid pRL-TK vector, which contains a cDNA encoding renilla luciferase (Promega Corporation, Madison, WI, USA) and 20 µg of reporter plasmid pNF-κB-Luc, which contains the firefly luciferase gene (Clonetech, Mountain View, CA, USA). The procedures followed have already been published (McClung et al, 2010).

Cytokine Enzyme-linked Immunosorbent Assay (ELISA). Protein levels of the cytokines tumor necrosis factor (TNF)-alpha, interferon-gamma, interleukin (IL)-6 and IL-1beta were quantified in the muscles of all study animals (diaphragms and gastrocnemius muscles) using specific sandwich ELISA kits eBiosience, Bender MedSystems, Vienna, Austria) following previously published methodologies (Barreiro et al, 2008;Barreiro et al, 2010b;Fermoselle et al, 2012).

Muscle fiber counts and morphometry. On 3-micrometer muscle paraffin-embedded sections from diaphragms and gastrocnemius muscles of all study groups, morphometrical analyses were performed as previously reported (Barreiro et al, 2010b;Barreiro et al, 2011;Fermoselle et al, 2012).

Muscle structure abnormalities. The area fraction of normal and abnormal muscle was evaluated on 3-micrometer paraffin-embedded sections of the diaphragm and gastrocnemius of all study groups following previously published methodologies (Figure E3) (Barreiro et al, 2010b;Barreiro et al, 2011;Fermoselle et al, 2012).

Terminal deoxynucleotidyl transferase-mediated dUTP nick-end labeling (TUNEL) assay. In muscle paraffin-embedded sections, apoptotic nuclei were identified using the TUNEL assay (In Situ Cell Death Detection Kit, POD**,** Roche Applied Science, Mannheim, Germany) in both diaphragms and gastrocnemius muscles from all study groups following precisely the manufacturer's instructions and previously published studies (Barreiro et al, 2011).

Statistical Analysis

Results are presented as mean (SD). Comparisons of physiological and biological variables among the different study groups were analyzed using one-way analysis of variance. For the purpose of the study two different sets of comparisons were made: i) control and LC cachectic mice, and on the other hand ii) LC cachectic and LC cachectic-bortezomib, iii) LC cachectic and LC cachectic-NF-κB inhibitor; and iv) LC cachectic and LC cachectic-MAPK inhibitor. Tukey's *post hoc* analysis was used to adjust for multiple comparisons. Statistical significance corresponding to these two different sets of comparisons is being specifically indicated in both Figures and Tables. Correlations between physiological and biological variables were explored using the Pearson's correlation coefficient. The sample size chosen was based on previous studies, where very similar approaches were employed (Barreiro et al, 2005;Barreiro et al, 2008;Barreiro et al, 2010b;Barreiro et al, 2011;Barreiro et al, 2012;Busquets et al, 2012;Diament et al, 2006;Fermoselle et al, 2011;Fermoselle et al, 2012;Marin-Corral et al, 2010;Muscaritoli et al, 2006;Penna et al, 2010;Testelmans et al, 2010;Troosters et al, 2010;Vogiatzis et al, 2010) and on assumptions of 80% power to detect an improvement of more than 20% in measured outcomes at a level of significance of $P \leq$

0.05. In most of the biological variables, mean difference between groups was initially estimated at a minimum of 20-25% and standard deviation was approximately 25-30% of the mean value for each of the variables.

RESULTS

Physiological characteristics

As shown in Table 1 and Figure 1, at the end of the study period (day 30), LC cachectic mice exhibited a reduction in body weight gain that was not observed in control animals. Food intake was similar among the study groups (3 g/24h). Diaphragm and gastrocnemius muscle weights and limb strength gain were significantly reduced in the LC cachectic mice compared to control rodents (Table 1). On day 15 (treatment period start point), mice did not show any statistically significant difference in body weight among the study groups (Table E1). LC cachectic mice treated with the NF-κB and MAPK inhibitors exhibited a significantly smaller reduction in weight gain, a significant improvement in diaphragm and gastrocnemius weight loss, and a significant recovery of muscle strength gain compared to the non-treated cachectic animals (Table 1). The progression of body weight during the study period for all the mouse groups is shown in Figure 1. The proteasome inhibitor did not induce any significant effects on body or muscle weights, or limb muscle strength in the LC cachectic mice (Table 1 and Figure 1). Importantly, the weight of the subcutaneous tumor was significantly reduced in the cachectic rodents treated with the inhibitors of the proteasome (18%), NF-κB (27%), and MAPK (60%) pathways compared to non-treated cachectic mice (Table 1).

10

Muscle proteolysis

Tyrosine release. Protein degradation, as measured by the release of the amino acid tyrosine, was increased in both diaphragm and gastrocnemius muscles of LC cachectic mice compared to controls (Figure 2A). Interestingly, treatment of cachectic mice with bortezomib, NF-κB, and MAPK inhibitor induced a significant reduction in tyrosine release levels in both respiratory and limb muscles (Figure 2A).

Proteolytic systems. The diaphragm muscle, but not gastrocnemius, of LC cachectic mice exhibited a significant increase in protein levels of calpain compared to controls (Table E2, Figure E4). The inhibitors of NF-κB and MAPK pathways elicited a significant reduction in calpain content only in the diaphragm of cachectic mice, while bortezomib did not induce any significant effect in any muscle (Table E2, Figure E4). Levels of the ubiquitin-conjugating enzyme $E2_{14\kappa}$ were increased only in the gastrocnemius of cachectic mice compared to controls (Figures 2B and E5). Importantly, inhibitors of proteasome, NF-κB, and MAPK pathways significantly decreased levels of $E2_{14k}$ in the gastrocnemius, but not the diaphragm, of cachectic mice (Figures 2B and E5). Levels of the E3 ligases atrogin-1 and MURF-1 did not differ in any muscle of the study groups (Table E2, Figures E6 and E7). Protein content of 20S proteasome subunit C8 did not differ between LC cachectic and control mice (Figure 2C, top panel, and Figure E8). As expected, bortezomib induced a significant reduction, especially in gastrocnemius, in protein content of subunit C8 among cachectic animals, while NF-κB and MAPK inhibitors did not elicit any significant modification (Figure 2C, top panel, and Figure E8). Protein ubiquitination levels were significantly greater in both respiratory and limb muscles of LC cachectic mice than in controls (Figure 2C, bottom panel, and Figure E9). In cachectic mice, bortezomib induced a significant reduction in protein ubiquination in both diaphragm and gastrocnemius, whereas NF-κB and MAPK inhibitors elicited a decrease in that proteolytic marker only in limb muscles (Figure 2C, bottom panel and Figure E9).

11

Signaling pathways of muscle proteolysis

FoxO pathway. While total content of FoxO-1 did not differ in any muscle between cachectic and control mice, content of p-FoxO-1 was significantly greater in gastrocnemius of cachectic rodents than in controls (Table E2 and Figures E10 and E11, respectively). Bortezomib induced a reduction in total FoxO-1 content, but not p-FoxO-1, only in cachectic diaphragms, whereas NF-κB and MAPK inhibitors did not elicit any modification in muscle content of either total or active FoxO-1 (Table E2 and Figures E10 and E11, respectively).

MAPK pathway. Muscle levels of MAPK subfamilies ASK1, ERK1/2, p-ERK1/2, JNK, and p-p38 did not differ between LC cachectic and control mice (Table E2 and Figures E12, E13, E14, E15, and E16, respectively). However, levels of total p38 were significantly greater in both diaphragm and gastrocnemius in cachectic mice than in controls (Table E2 and Figure E17). Interestingly, treatment of cachectic animals with MAPK inhibitor elicited a significant reduction in protein levels of ERK1/2, p-ERK1/2, and total p38 in respiratory and limb muscles (Table E2 and Figures E13, E14, and E17, respectively).

NF-κB pathway. In respiratory and limb muscles, protein content of p50 and p-p50 was significantly increased in cachectic animals compared to controls (Figures 3A, top and bottom panels, and Figures E18, and E19). A significant decrease was observed in total p50 in both diaphragm and gastrocnemius of cachectic mice in response to proteasome, NF-κB, and MAPK inhibitors, while p-p50 levels were only reduced in both muscles among animals treated with the NF-κB inhibitor controls (Figures 3A, top and bottom panels, and Figures E18, and E19). Total protein content of p65, but not p-p65, were increased in diaphragms and gastrocnemius of cachectic mice compared to controls (Figure 3B, top and bottom panels, and Figures E20 and E21). A significant reduction was detected in protein content of p65 in both respiratory and limb muscles of cachectic rodents in response to proteasome and NF-κB inhibitors, while p-p65 protein levels were decreased only in response to NF-κB inhibitor in

those muscles (Figure 3B, top and bottom panels, respectively, and Figures E20 and E21). Protein levels of total IκB and p-IκB were significantly diminished in both diaphragms and gastrocnemius muscles in cachectic mice compared to controls (Figure 3C top and bottom panels, and Figures E22 and E23). Interestingly, treatment of cachectic rodents with proteasome, NF-κB, and MAPK inhibitors elicited an increase in both total IκB and p-IκB markers in respiratory (except for MAPK inhibitor) and limb muscles Figure 3C top and bottom panels, respectively, and Figures E22 and E23). Transcriptional activity of NF-κB was increased in cachectic mice compared to controls (Figure 3D). Importantly, among cachectic rodents, treatment with both proteasome and NF-κB inhibitors elicited a significant decline in NF-κB transcriptional activity, while no differences were observed in response to MAPK inhibition (Figure 3D).

Muscle growth and differentiation. In cachectic mice, protein levels of myostatin were increased in both diaphragms and gastrocnemius compared to control rodents (Figures 4A and E24). Importantly, proteasome, NF-κB, and MAPK inhibitors elicited a significant reduction in myostatin levels in muscles of cachectic animals (Figures 4A, top panel, and E24). Nevertheless, compared to controls, protein content of myogenin was significantly reduced within respiratory and limb muscles of cachectic rodents, while treatment with either NF-κB or MAPK inhibitors, but not bortezomib, elicited a rise in myogenin content in their muscles (Figures 4A, bottom panel, and E25).

Contractile and functional muscle proteins

Protein levels of contractile MyHC were reduced in diaphragm and gastrocnemius of cachectic mice compared to controls (Figure 4B, top panel). Interestingly, NF-κB and MAPK inhibitors, but not bortezomib, elicited an improvement in MyHC protein content in respiratory and limb muscles among cachectic rodents (Figures 4B, top panel, and E26). Protein content of skeletal muscle actin did not differ among any of the study groups (Figures

13

4B, bottom panel, and E27). Compared to controls, creatine kinase protein content was significantly reduced only in gastrocnemius of tumor-bearing animals (Table E2 and Figure 28). Treatment of these mice with proteasome, NF-κB, and MAPK inhibitors induced a rise in creatine kinase content only in limb muscles (Table E2 and Figure E28). No differences were detected in carbonic anhydrase-3 muscle levels among the study groups (Table E2 and Figures E29).

Muscle inflammation and redox balance

Inflammatory cytokines. ELISA levels of interferon-gamma were only significantly increased in diaphragms of cachectic mice compared to controls (Table E2). TNF-alpha, IL-6, and IL-1beta ELISA levels did not differ between cachectic and control mice (Table E2). Treatment with bortezomib elicited a significant decline in protein levels of interferon-gamma, TNF-alpha, IL-6, and IL-1beta in gastrocnemius of cachectic rodents (Table E2). Protein content of the studied cytokines was not different in any muscles of cachectic animals in response to NF-κB inhibition (Table E2). Diaphragm levels of interferon-gamma, TNF-alpha, and IL-6 were decreased among cachectic rodents treated with MAPK inhibitor (Table E2).

Oxidative stress markers. Compared to controls, protein carbonylation levels were significantly increased in both diaphragms and gastrocnemius muscles of cachectic mice (Table E2 and Figure E30). Treatment of these rodents with proteasome, NF-κB, and MAPK inhibitors elicited a reduction in total protein carbonylation in respiratory and limb muscles (Table E2 and Figure E30). HNE-protein adduct levels were increased only in gastrocnemius of tumor-bearing mice compared to controls, and treatment with proteasome, NF-κB, and MAPK inhibitors did not induce any significant effect on their muscles (Table E2 and Figure E31). Muscle protein tyrosine nitration levels did not differ among the study groups (Table E2 and Figure E32).

Antioxidant enzymes. Compared to control rodents, protein levels of SOD2 were decreased in

diaphragms and gastrocnemius of tumor-bearing mice, and treatment with proteasome, NF-κB, and MAPK inhibitors elicited a significant rise in SOD2 content only in gastrocnemius (Table E2 and Figure E33). Muscle protein content of CuZn-SOD and catalase did not differ among study groups (Table E2, and Figures E34 and E35, respectively).

Muscle autophagy

Muscle protein levels of the autophagy system p62 and beclin-1 did not differ among the study groups (Table E2, and Figures E36 and E37). Protein levels of LC3 as measured by the ratio of LC3-II to LC3-I, however, were significantly increased in diaphragm and gastrocnemius of cachectic mice compared to controls (Figures 5 and E38), and treatment with proteasome, NF-κB, or MAPK inhibitors elicited a significant decline in LC3II/LC in diaphragms and gastrocnemius of tumor-bearing mice (Figures 5 and E38).

Muscle structure

Fiber type composition. Proportions of type I and type II fibers were not different in any muscle among the study groups (Table 2). Compared to controls, the size of slow- and fast-twitch fibers was significantly diminished in both diaphragm and gastrocnemius of cachectic mice (Table 2 and Figures 6A and 6B). In these animals, treatment with either proteasome or MAPK inhibitors, but not NF-κB inhibitor, elicited a significant improvement in sizes of type I fibers in both muscles (Table 2 and Figures 6A and 6B).

Muscle abnormalities. Compared to control mice, proportions of abnormal muscle were greater in both diaphragms and gatrocnemius of cachectic animals (Table 2). In these animals, treatment with MAPK inhibitor elicited a significant reduction in total muscle abnormalities only in the limb muscle, while inducing a decrease in inflammatory cell proportions in both muscles (Table 2). Compared to controls, TUNEL-stained nuclei counts were increased in both diaphragms and gastrocnemius of cachectic mice (Table 2 and Figures 6C and 6D). Importantly, only treatment of these animals with MAPK inhibitor induced a significant

decrease in proportions of TUNEL-stained nuclei in their diaphragms (Table 2 and Figures 6C and 6D).

DISCUSSION

In BALB/c mice, subcutaneous inoculation of LP07 cells induced lung metastases, together with a severe cachexia that was accompanied by a significant decline in the diaphragm and limb muscle mass and strength generation (Urtreger et al, 2001). Despite that a recent investigation (Roberts et al, 2013) elegantly showed that colon-26 cancer cachexia is characterized by diaphragm muscle structure and function impairment in mice, we believe that the current findings on proteolysis, signaling pathways, and structural alterations add insight into current knowledge on how several muscle types are affected in the process of muscle wasting. Moreover, it also sheds light on the predominant role of MAPK and NF-κB signaling in the process of muscle wasting, which could be targeted with pharmacological agents. In fact, knowledge on the treatment of muscle wasting is still at its infancy and additional confirmatory studies are needed, especially in cancer cachexia, which is further impaired by chemotherapy (Garcia et al, 2013;Hajjaji et al, 2012;Xue et al, 2011). Previous investigations showed that nutrition modulation using several nutrients (Hajjaji et al, 2012;Xue et al, 2011) and ghrelin (Garcia et al, 2013) may prevent body weight loss in cancer patients undergoing chemotherapy. Moreover, the metabolic modulator trimetazidine was also shown to activate protein synthesis signaling, while decreasing E3 ligase and myostatin levels in experimental models (Ferraro et al, 2013). The current study focuses on the assessment of the effects of several inhibitors of key cellular pathways in experimental cancer-induced cachexia.

16

In line with the study hypothesis, the main findings in the investigation were that compared to control animals, in both respiratory and limb muscles of LC cachectic mice: 1) muscle proteolysis was enhanced; 2) total amounts of ubiquitinated proteins and autophagy were increased; 3) calpain levels were higher only in the diaphragm; 4) myostatin levels were greater, while those of myogenin were reduced; 5) protein creatine kinase levels were decreased only in the gastrocnemius; 6) levels of contractile MyHC were reduced, while those of actin were not modified; 7) the size of slow- and fast-twitch muscle fibers was decreased in both muscles, while proportions of muscle abnormalities and TUNEL-stained nuclei were increased; 8) protein oxidation levels were greater, whereas inflammatory cytokine levels were not modified; and 9) signaling pathways such as FoxO-1, NF-κB, and MAPK were increased. Treatment of LC cachectic mice with the pharmacological inhibitors induced several modifications that are discussed below.

Pharmacological proteasome inhibition in cancer cachectic muscles

Proteasome, an energy-dependent proteolytic system, is a key modulator of cellular processes including NF-κB signaling and is also involved in cell metabolism and DNA repair. Among the different pharmacological proteasome inhibitors described so far, bortezomib is currently the only agent approved for clinical use in patients with cancer(Cvek and Dvorak, 2007). Proteasome also seems to play a major role in the muscle mass loss and dysfunction process associated with several chronic conditions(Supinski et al, 2009;van Hees et al, 2008;van et al, 2011) and severe infections(Roth et al, 2005).

In the current investigation, although cachectic mice treated with bortezomib exhibited a significantly lower tumor size compared to non-treated tumor-bearing rodents, body and muscle weights together with limb muscle force did not improve. In fact, only an improvement in the size of slow-twitch fibers, but not type II, was observed in either respiratory or limb muscles in response to proteasome inhibition. Besides, no significant modifications in contractile MyHC or actin contents were detected in any muscle. These

17

findings are in agreement with those reported in a previous study conducted in endotoxemic rats (Supinski et al, 2009), in which treatment with several proteasome inhibitors prevented muscle proteolysis, but not diaphragm muscle loss or force generation. Nevertheless, the present findings and those previously reported (Supinski et al, 2009), are counter to results demonstrated in other two investigations, in which contractile diaphragm function was shown to improve in response to bortezomib in rats bearing congestive heart failure (van Hees et al, 2008) and emphysema (van et al, 2011).

One likely explanation to account for differences encountered among studies (Supinski et al, 2009;van Hees et al, 2008;van et al, 2011) is that different proteolytic systems other than the proteasome may participate in reduced body weight, and decreased muscle mass and weakness under several experimental conditions. In line with this, it was demonstrated (Fareed et al, 2006;Supinski and Callahan, 2006) that other proteases such as caspase and calpain (not modified by bortezomib in any muscle) need to be initially activated within the myocytes in order to break down the contractile myofilaments under muscle wasting conditions. Moreover, the proteasome inhibitor seems to have rather prevented proteolysis (lower tyrosine release levels and tumor sizes) of non-contractile proteins (cytosolic or nuclear proteins), which may account for the lack of significant improvements observed in limb muscle function, and in both myofibrilar protein and muscle mass loss in this experimental model of cancer cachexia. Another explanation accounting for the failure of bortezomib to improving muscle mass or function in the cachectic mice is the lack of effects of the proteasome inhibitor on muscle protein synthesis. This pathway is likely to be reduced in the muscles of the cachectic mice, as was shown to occur in other models of cancer-induced cachexia (Robert et al, 2012). However, the present investigation was not designed to explore protein anabolism in the mouse cachectic muscles. Another interesting finding in the investigation was the reduction in protein content of the 20S proteasome subunit in both respiratory and limb muscles in response to bortezomib, which was not induced by the other

18

agents. It is likely that chronic administration (15 days) of the proteasome inhibitor may also induce and effect not only on proteasome activity but also on its content.

Pharmacological NF-κB inhibition in cancer cachectic muscles

NF-κB modulates the expression of cytokines, growth factors, and a wide variety of genes that regulate physiological and pathological conditions. NF-κB is one of the most relevant signaling pathways leading to skeletal muscle loss. It is composed by a family of five members (p65, Rel-B, c-Rel, p50, and p52), which are all expressed within skeletal muscles. The NF-κB dimers RelA (p65) and NF-κB1 (p50) are sequestered in an active cytoplasmic complex by binding to its inhibitory subunit IκB. Following the stimulus, IκB becomes phosphorylated by specific kinases. This phosphorylation entails ubiquitination and fast degradation of IκB by the proteasome. Free NF-κB dimers translocate to the nucleus and activate target genes. Sulfasalazine was shown to be a powerful and specific NF-κB inhibitor by essentially inhibiting NF-κB-dependent transcription in several models (Camara-Lemarroy et al, 2009;Olmez et al, 2008;Wahl et al, 1998).

In the current investigation, it has been clearly demonstrated that NF-κB pathway was upregulated in both respiratory and limb muscles of LC cachectic mice. In those muscles, sulfasalazine elicited a significant decline in protein levels of total and phosphorylated p65 and p50 members, while inducing a substantial upregulation of IκB and p-IκB among the cachectic rodents. Moreover, in the present experimental model, these findings were further confirmed by experiments performed to specifically assess NF-κB transcriptional activity. In this regard, NF-κB activity was increased in diaphragm and gastrocnemius muscles of cachectic mice, whereas the activity was specifically downregulated in response to both proteasome and NF-κB inhibition, especially the latter. These are interesting findings which suggest that NF-κB plays a crucial role in cancer-induced cachexia signaling in this

experimental model of cancer cachexia.

Importantly, treatment of the cachectic mice with sulfasalazine also elicited other interesting modifications in muscles of the cachectic rodents. In this respect, a substantial improvement was seen in body and muscle weights, limb muscle strength, and tumor size (27% decrease), together with a reduction in muscle protein degradation and oxidation, $E2_{14\kappa}$ and protein ubiquitination levels, myostatin content, and autophagy as measured by LC3-II/LC3-I levels. Additionally, in muscles of tumor-bearing mice treated with sulfasalazine, a significant increase in myogenin, contractile MyHC, and creatine kinase content, was also observed in response to NF-κB inhibition. Protein levels of SOD2 were also increased in the limb muscles, but not the diaphragm, of the cachectic mice in response to sulfasalazine. These findings are counter to previous studies in which NF-κB activity was shown to induce SOD2 expression (Rui and Kvietys, 2005;Sundaramoorthy et al, 2013). Differences in the experimental models and cell types may account for discrepancies between the studies (Rui and Kvietys, 2005;Sundaramoorthy et al, 2013). No significant modifications, however, were seen in fiber sizes or muscle cytokine content, whose levels were, indeed, similar to those observed in the muscles of the non-treated cachectic and control animals. This is somehow counter to previous reports (Peterson et al, 2011), in which NF-κB and TNF-alpha were shown to signal muscle atrophy. Moreover, it is likely that NF-κB pathway predominantly regulates apoptosis and nonimmune autophagy in multinucleated cells as shown in other models (Alger et al, 2011). This observation may account for the lack of improvement observed in the muscle fibers sizes in response to NF-κB pathway inhibition in the cachectic mice (Alger et al, 2011).

Body and muscle weight and strength improvement in response to NF-κB inhibition was likely to be achieved through the contribution of several factors such as reduced levels of protein degradation, myostatin, and autophagy, and increased myogenin content, which may

have led, in turn, to higher content of contractile MyHC in the cachectic muscles. Myostatin, which is almost exclusively expressed in skeletal muscles, is a potent negative regulator of muscle mass. The increase in myostatin levels observed in the cachectic muscles are in line with previous reports, in which significant increases in myostatin content were shown in diaphragm and gastrocnemius of emphysema cachectic mice (Fermoselle et al, 2011), in muscles of cachectic COPD patients (Fermoselle et al, 2012;Testelmans et al, 2010;Troosters et al, 2010;Vogiatzis et al, 2010), and in cancer patients (Aversa et al, 2012). A thorough assessment of the myostatin and activin IIB system was not the focus of the current research. Nonetheless, previous investigations have clearly demonstrated that the sActRIIB led to an improvement in muscle mass loss, exercise, and survival in cachectic mice (Busquets et al, 2012;Zhou et al, 2010).

Myogenin plays an important role in skeletal muscle differentiation, maintenance and repair, regulating muscle metabolism and energy utilization. Levels of myogenin were decreased in muscles of the cachectic mice, while NF-κB restored those levels in both muscles. These findings are in keeping with a previous investigation (Fermoselle et al, 2012;Testelmans et al, 2010;Troosters et al, 2010;Vogiatzis et al, 2010), in which myogenin levels were also decreased in cachectic severe COPD patients. Another aspect that deserves attention is the smaller size of the subcutaneous tumor in response to NF-κB inhibition among the LC cachectic mice. However, the present investigation was not designed to disentangle the potential relationships between tumor size and the degree of cachexia in the animals.

Pharmacological MAPK inhibition in cancer cachectic muscles

MAPK cascade leads to the activation of protein kinases and transcription factors through phosphorylation, resulting in signal transduction, hence playing a key role in cell signaling. In the current study, both total and phosphorylated protein content of the best characterized MAPK subfamilies ERK1/2, p38, JNK, and ASK1 was explored in the muscles of all groups of mice. Total p38, but not p-p38, levels were increased in both respiratory and limb muscles

21

of tumor-bearing rodents. Importantly, MAPK inhibition elicited a significant improvement in body and muscle weight gain, limb strength, proteolysis and protein ubiquitination levels, especially in the gastrocnemius. These findings are in line with a recent investigation in which muscle mass loss was restored by inhibiting ERK activity in colon cancer mice (Penna et al, 2010).

MAPK inhibition was confirmed by the significant decrease in protein content of both total and phosphorylated ERK1/2 in respiratory and limb cachectic muscles. Additionally, MAPK inhibitor elicited a significant decrease in p38 protein content in diaphragm and limb muscles of tumor-bearing rodents. Importantly, inhibition of MAPK pathway also induced other interesting findings in the cachectic animals such as an increase in myogenin content together with a reduction in myostatin levels, a substantial rise in contractile MyHC in both diaphragm and gastrocnemius, an increase in creatine kinase protein in the limb muscle, and a decrease in protein oxidation and autophagy levels in both muscles. Interestingly, from a structural standpoint, cachectic mice treated with MAPK inhibitor also exhibited larger slow-twitch muscle fibers in diaphragm and gastrocnemius along with a decrease in the percentage of muscle structural abnormalities.

Taken together, these findings suggest that MAPK pathway controls muscle proteolysis through the ubiquitin-proteasome and autophagy systems in both respiratory and limb muscles of cancer cachectic mice. Other mechanisms involved in the regulation of muscle mass such as myostatin and myogenin were also modulated by the effect of MAPK inhibitor in the cachectic muscles. Finally, an interesting finding in the current study is the substantial reduction in tumor size (60%) observed in tumor-bearing mice treated with the MAPK inhibitor. As abovementioned, a significant reduction in tumor size might have also contributed to attenuating the cachectic effects in the muscles of the treated mice. We do not believe, however, that this phenomenon has been a relevant contributor in the investigation for the following reason. The effects of NF-κB inhibition on the size of the subcutaneous

22

tumor were smaller compared to those elicited by MAPK inhibitor and relatively similar to those elicited by bortezomib, while a greater modulation of body weight and muscle mass and force development was achieved in response to NF-κB than to MAPK or proteasome inhibitions. Future studies may be designed in order to specifically address to what extent tumor size and regulation by pharmacological agents contribute to muscle wasting and weakness in cancer-induced cachexia.

Finally, another relevant finding in the investigation was the increased protein oxidation levels encountered in respiratory and limb cachectic muscles. Inhibition of proteasome, NF-κB, and MAPK activities elicited a significant decline in protein carbonylation in diaphragm and gastrocnemius muscles. Indeed, NF-κB and MAPK activation seem to play a relevant role in the transcriptional regulation of redox balance within muscles, while also mediating oxidative stress-induced muscle atrophy (McClung et al, 2010;Powers et al, 2005).

Study limitations and future perspectives

A first limitation is related to the lack of measurements on the tumor size throughout the entire duration of the protocol in the tumor-bearing animals. In the study, tumor weights were only available at the time of sacrifice in all experimental groups. Another limitation has to do with the lack of specific functional data on the diaphragm muscle. However, a first step in this field of investigation was to explore whether molecular and cellular events involved in muscle wasting also take place in the main respiratory muscle in an experimental model of cancer cachexia. Besides, a previous study already showed that muscle contractile function was severely affected in another model of cachexia in mice (Roberts et al, 2013).

Additionally, the reduction in tumor burden observed in the cachectic rodents in response to treatment with the pharmacological inhibitors could have also influenced the molecular events found in the muscles. In this regard, tumor growth as measured by ki-67 (cell proliferation marker) decreased in the cachectic mice treated with any of the inhibitors (data not shown). Future investigations should elucidate to what extent these specific

23

inhibitors partly act via a reduction in tumor burden and growth or mostly exert a direct effect on the muscle fibers.

Despite the relevance of the current findings in the attenuation of muscle wasting, results should be taken cautiously in clinical settings of patients with cancer cachexia, as the studied pharmacological agents may also exert effects on other tissues and organs. The identification of more tissue-specific inhibitors or selective devices to deliver the drugs to the target organs warrants further research.

Finally, it should be mentioned that exercise capacity, physical activity, or fatigue resistance may additionally provide valuable information in this specific model of LC cachexia despite that they were not explored in the current study. However, previous investigations based on the utilization of similar models of cancer cachexia, limb muscle strength was indeed the main physiological end-point (Murphy et al, 2012;Toledo et al, 2011;Whittemore et al, 2003). In summary, several questions remain unanswered, which will have to be addressed in future studies aimed to explore those specific issues in experimental models of cachexia.

Conclusions

We conclude from the present experimental model of LC-induced cachexia that NF-κB and MAPK are predominant signaling pathways. Pharmacological inhibition of NF-κB and MAPK, but not the proteasome system, induced in cancer cachectic animals, a substantial restoration of muscle mass and force through a decrease in muscle protein oxidation and catabolism, myostatin, and autophagy, together with a greater content in myogenin, and contractile and functional proteins. Attenuation of MAPK and NF-κB signaling pathways exerts beneficial effects on muscles in cancer-induced cachexia, thus offering potential new therapeutic strategies for this condition.

ACKNOWLEDGMENTS

CONFLICT OF INTEREST

The authors declare no conflict of interest in relation to this study.

Literature Cited

Agusti A, Morla M, Sauleda J, Saus C, Busquets X (2004). NF-kappaB activation and iNOS upregulation in skeletal muscle of patients with COPD and low body weight. Thorax 59:483-487.

Alger HM, Raben N, Pistilli E, Francia DL, Rawat R, Getnet D, Ghimbovschi S, Chen YW, Lundberg IE, Nagaraju K (2011). The role of TRAIL in mediating autophagy in myositis skeletal muscle: a potential nonimmune mechanism of muscle damage. Arthritis Rheum 63:3448-3457.

Argiles JM, Busquets S, Lopez-Soriano FJ (2011). Anti-inflammatory therapies in cancer cachexia. Eur J Pharmacol 668 Suppl 1:S81-S86.

Argiles JM, Lopez-Soriano FJ (1996). The ubiquitin-dependent proteolytic pathway in skeletal muscle: its role in pathological states. Trends Pharmacol Sci 17:223-226.

Aversa Z, Bonetto A, Penna F, Costelli P, Di RG, Lacitignola A, Baccino FM, Ziparo V, Mercantini P, Rossi FF, Muscaritoli M (2012). Changes in myostatin signaling in non-weight-losing cancer patients. Ann Surg Oncol 19:1350-1356.

Barreiro E, de la PB, Busquets S, Lopez-Soriano FJ, Gea J, Argiles JM (2005). Both oxidative and nitrosative stress are associated with muscle wasting in tumour-bearing rats. FEBS Lett 579:1646-1652.

Barreiro E, Del Puerto-Nevado L, Puig-Vilanova E, Perez-Rial S, Sanchez F, Martinez-Galan L, Rivera S, Gea J, Gonzalez-Mangado N, Peces-Barba G (2012). Cigarette smoke-induced oxidative stress in skeletal muscles of mice. Respir Physiol Neurobiol 182:9-17.

Barreiro E, Ferrer D, Sanchez F, Minguella J, Marin-Corral J, Martinez-Llorens J, Lloreta J, Gea J (2011). Inflammatory cells and apoptosis in respiratory and limb muscles of patients with COPD. J Appl Physiol 111:808-817.

Barreiro E, Garcia-Martinez C, Mas S, Ametller E, Gea J, Argiles JM, Busquets S, Lopez-Soriano FJ (2009). UCP3 overexpression neutralizes oxidative stress rather than nitrosative stress in mouse myotubes. FEBS Lett 583:350-356.

Barreiro E, Marin-Corral J, Sanchez F, Mielgo V, Alvarez FJ, Galdiz JB, Gea J (2010a). Reference values of respiratory and peripheral muscle function in rats. J Anim Physiol Anim Nutr (Berl) 94:e393-e401.

Barreiro E, Peinado VI, Galdiz JB, Ferrer E, Marin-Corral J, Sanchez F, Gea J, Barbera JA (2010b). Cigarette smoke-induced oxidative stress: A role in chronic obstructive pulmonary disease skeletal muscle dysfunction. Am J Respir Crit Care Med 182:477-488.

Barreiro E, Schols AM, Polkey MI, Galdiz JB, Gosker HR, Swallow EB, Coronell C, Gea J (2008). Cytokine profile in quadriceps muscles of patients with severe COPD. Thorax 63:100-107.

Busquets S, Toledo M, Orpi M, Massa D, Porta M, Capdevila E, Padilla N, Frailis V, Lopez-Soriano FJ, Han HQ, Argiles JM (2012). Myostatin blockage using actRIIB antagonism in mice bearing the Lewis lung carcinoma results in the improvement of muscle wasting and physical performance. J Cachexia Sarcopenia Muscle 3:37-43.

Cai D, Frantz JD, Tawa NE, Jr., Melendez PA, Oh BC, Lidov HG, Hasselgren PO, Frontera WR, Lee J, Glass DJ, Shoelson SE (2004). IKKbeta/NF-kappaB activation causes severe muscle wasting in mice. Cell 119:285-298.

Camara-Lemarroy CR, Guzman-de la Garza FJ, Alarcon-Galvan G, Cordero-Perez P, Fernandez-Garza NE (2009). Effect of sulfasalazine on renal ischemia/reperfusion injury in rats. Ren Fail 31:822-828.

Cvek B, Dvorak Z (2007). Targeting of nuclear factor-kappaB and proteasome by dithiocarbamate complexes with metals. Curr Pharm Des 13:3155-3167.

Diament MJ, Garcia C, Stillitani I, Saavedra VM, Manzur T, Vauthay L, Klein S (1998). Spontaneous murine lung adenocarcinoma (P07): A new experimental model to study paraneoplastic syndromes of lung cancer. Int J Mol Med 2:45-50.

Diament MJ, Peluffo GD, Stillitani I, Cerchietti LC, Navigante A, Ranuncolo SM, Klein SM (2006). Inhibition of tumor progression and paraneoplastic syndrome development in a murine lung adenocarcinoma by medroxyprogesterone acetate and indomethacin. Cancer Invest 24:126-131.

Evans WJ, Morley JE, Argiles J, Bales C, Baracos V, Guttridge D, Jatoi A, Kalantar-Zadeh K, Lochs H, Mantovani G, Marks D, Mitch WE, Muscaritoli M, Najand A, Ponikowski P, Rossi FF, Schambelan M, Schols A, Schuster M, Thomas D, Wolfe R, Anker SD (2008). Cachexia: a new definition. Clin Nutr 27:793-799.

Fareed MU, Evenson AR, Wei W, Menconi M, Poylin V, Petkova V, Pignol B, Hasselgren PO (2006). Treatment of rats with calpain inhibitors prevents sepsis-induced muscle proteolysis independent of atrogin-1/MAFbx and MuRF1 expression. Am J Physiol Regul Integr Comp Physiol 290:R1589-R1597.

Fermoselle C, Rabinovich R, Ausin P, Puig-Vilanova E, Coronell C, Sanchez F, Roca J, Gea J, Barreiro E (2012). Does oxidative stress modulate limb muscle atrophy in severe COPD patients? Eur Respir J 40:851-862.

Fermoselle C, Sanchez F, Barreiro E (2011). [Reduction of muscle mass mediated by myostatin in an experimental model of pulmonary emphysema]. Arch Bronconeumol 47:590-598.

Ferraro E, Giammarioli AM, Caldarola S, Lista P, Feraco A, Tinari A, Salvatore AM, Malorni W, Berghella L, Rosano G (2013). The metabolic modulator trimetazidine triggers autophagy and counteracts stress-induced atrophy in skeletal muscle myotubes. FEBS J 280:5094-5108.

Garcia JM, Scherer T, Chen JA, Guillory B, Nassif A, Papusha V, Smiechowska J, Asnicar M, Buettner C, Smith RG (2013). Inhibition of cisplatin-induced lipid catabolism and weight loss by ghrelin in male mice. Endocrinology 154:3118-3129.

Hajjaji N, Couet C, Besson P, Bougnoux P (2012). DHA effect on chemotherapy-induced body weight loss: an exploratory study in a rodent model of mammary tumors. Nutr Cancer 64:1000-1007.

Kramer HF, Goodyear LJ (2007). Exercise, MAPK, and NF-kappaB signaling in skeletal muscle. J Appl Physiol 103:388-395.

Lu C, Gallegos R, Li P, Xia CQ, Pusalkar S, Uttamsingh V, Nix D, Miwa GT, Gan LS (2006). Investigation of drug-drug interaction potential of bortezomib in vivo in female Sprague-Dawley rats and in vitro in human liver microsomes. Drug Metab Dispos 34:702-708.

Marin-Corral J, Fontes CC, Pascual-Guardia S, Sanchez F, Olivan M, Argiles JM, Busquets S, Lopez-Soriano FJ, Barreiro E (2010). Redox balance and carbonylated proteins in limb and heart muscles of cachectic rats. Antioxid Redox Signal 12:365-380.

Mastrocola R, Reffo P, Penna F, Tomasinelli CE, Boccuzzi G, Baccino FM, Aragno M, Costelli P (2008). Muscle wasting in diabetic and in tumor-bearing rats: role of oxidative stress. Free Radic Biol Med 44:584-593.

McClung JM, Judge AR, Powers SK, Yan Z (2010). p38 MAPK links oxidative stress to autophagy-related gene expression in cachectic muscle wasting. Am J Physiol Cell Physiol 298:C542-C549.

Moore-Carrasco R, Busquets S, Almendro V, Palanki M, Lopez-Soriano FJ, Argiles JM (2007). The AP-1/NF-kappaB double inhibitor SP100030 can revert muscle wasting during

experimental cancer cachexia. Int J Oncol 30:1239-1245.

Morley JE, Argiles JM, Evans WJ, Bhasin S, Cella D, Deutz NE, Doehner W, Fearon KC, Ferrucci L, Hellerstein MK, Kalantar-Zadeh K, Lochs H, MacDonald N, Mulligan K, Muscaritoli M, Ponikowski P, Posthauer ME, Rossi FF, Schambelan M, Schols AM, Schuster MW, Anker SD (2010). Nutritional recommendations for the management of sarcopenia. J Am Med Dir Assoc 11:391-396.

Murphy KT, Chee A, Trieu J, Naim T, Lynch GS (2012). Importance of functional and metabolic impairments in the characterization of the C-26 murine model of cancer cachexia. Dis Model Mech 5:533-545.

Muscaritoli M, Bossola M, Aversa Z, Bellantone R, Rossi FF (2006). Prevention and treatment of cancer cachexia: new insights into an old problem. Eur J Cancer 42:31-41.

Olmez D, Babayigit A, Uzuner N, Erbil G, Karaman O, Yilmaz O, Cetin EO, Ozogul C (2008). Efficacy of sulphasalazine on lung histopathology in a murine model of chronic asthma. Exp Lung Res 34:501-511.

Penna F, Costamagna D, Fanzani A, Bonelli G, Baccino FM, Costelli P (2010). Muscle wasting and impaired myogenesis in tumor bearing mice are prevented by ERK inhibition. PLoS One 5:e13604.

Penner CG, Gang G, Wray C, Fischer JE, Hasselgren PO (2001). The transcription factors NF-kappab and AP-1 are differentially regulated in skeletal muscle during sepsis. Biochem Biophys Res Commun 281:1331-1336.

Peterson JM, Bakkar N, Guttridge DC (2011). NF-kappaB signaling in skeletal muscle health and disease. Curr Top Dev Biol 96:85-119.

Powers SK, Kavazis AN, DeRuisseau KC (2005). Mechanisms of disuse muscle atrophy: role of oxidative stress. Am J Physiol Regul Integr Comp Physiol 288:R337-R344.

Robert F, Mills JR, Agenor A, Wang D, DiMarco S, Cencic R, Tremblay ML, Gallouzi IE, Hekimi S, Wing SS, Pelletier J (2012). Targeting protein synthesis in a Myc/mTOR-driven model of anorexia-cachexia syndrome delays its onset and prolongs survival. Cancer Res 72:747-756.

Roberts BM, Ahn B, Smuder AJ, Al-Rajhi M, Gill LC, Beharry AW, Powers SK, Fuller DD, Ferreira LF, Judge AR (2013). Diaphragm and ventilatory dysfunction during cancer cachexia. FASEB J 27:2600-2610.

Roth GA, Moser B, Krenn C, Roth-Walter F, Hetz H, Richter S, Brunner M, Jensen-Jarolim E, Wolner E, Hoetzenecker K, Boltz-Nitulescu G, Ankersmit HJ (2005). Heightened levels of circulating 20S proteasome in critically ill patients. Eur J Clin Invest 35:399-403.

Rui T, Kvietys PR (2005). NFkappaB and AP-1 differentially contribute to the induction of Mn-SOD and eNOS during the development of oxidant tolerance. FASEB J 19:1908-1910.

Schuh K, Pahl A (2009). Inhibition of the MAP kinase ERK protects from lipopolysaccharide-induced lung injury. Biochem Pharmacol 77:1827-1834.

Smith HJ, Tisdale MJ (2003). Signal transduction pathways involved in proteolysis-inducing

factor induced proteasome expression in murine myotubes. Br J Cancer 89:1783-1788.

Sundaramoorthy S, Ryu MS, Lim IK (2013). B-cell translocation gene 2 mediates crosstalk between PI3K/Akt1 and NFkappaB pathways which enhances transcription of MnSOD by accelerating IkappaBalpha degradation in normal and cancer cells. Cell Commun Signal 11:69.

Supinski GS, Callahan LA (2006). Caspase activation contributes to endotoxin-induced diaphragm weakness. J Appl Physiol 100:1770-1777.

Supinski GS, Vanags J, Callahan LA (2009). Effect of proteasome inhibitors on endotoxin-induced diaphragm dysfunction. Am J Physiol Lung Cell Mol Physiol 296:L994-L1001.

Testelmans D, Crul T, Maes K, Agten A, Crombach M, Decramer M, Gayan-Ramirez G (2010). Atrophy and hypertrophy signalling in the diaphragm of patients with COPD. Eur Respir J 35:549-556.

Tischler ME, Desautels M, Goldberg AL (1982). Does leucine, leucyl-tRNA, or some metabolite of leucine regulate protein synthesis and degradation in skeletal and cardiac muscle? J Biol Chem 257:1613-1621.

Toledo M, Busquets S, Sirisi S, Serpe R, Orpi M, Coutinho J, Martinez R, Lopez-Soriano FJ, Argiles JM (2011). Cancer cachexia: physical activity and muscle force in tumour-bearing rats. Oncol Rep 25:189-193.

Troosters T, Probst VS, Crul T, Pitta F, Gayan-Ramirez G, Decramer M, Gosselink R (2010). Resistance training prevents deterioration in quadriceps muscle function during acute exacerbations of chronic obstructive pulmonary disease. Am J Respir Crit Care Med 181:1072-1077.

Urtreger AJ, Diament MJ, Ranuncolo SM, Del C, V, Puricelli LI, Klein SM, De Kier Joffe ED (2001). New murine cell line derived from a spontaneous lung tumor induces paraneoplastic syndromes. Int J Oncol 18:639-647.

van Hees HW, Li YP, Ottenheijm CA, Jin B, Pigmans CJ, Linkels M, Dekhuijzen PN, Heunks LM (2008). Proteasome inhibition improves diaphragm function in congestive heart failure rats. Am J Physiol Lung Cell Mol Physiol 294:L1260-L1268.

van HH, Ottenheijm C, Ennen L, Linkels M, Dekhuijzen R, Heunks L (2011). Proteasome inhibition improves diaphragm function in an animal model for COPD. Am J Physiol Lung Cell Mol Physiol 301:L110-L116.

Vignaud A, Ferry A, Huguet A, Baraibar M, Trollet C, Hyzewicz J, Butler-Browne G, Puymirat J, Gourdon G, Furling D (2010). Progressive skeletal muscle weakness in transgenic mice expressing CTG expansions is associated with the activation of the ubiquitin-proteasome pathway. Neuromuscul Disord 20:319-325.

Vogiatzis I, Simoes DC, Stratakos G, Kourepini E, Terzis G, Manta P, Athanasopoulos D, Roussos C, Wagner PD, Zakynthinos S (2010). Effect of pulmonary rehabilitation on muscle remodelling in cachectic patients with COPD. Eur Respir J 36:301-310.

von HS, Anker SD (2010). Cachexia as a major underestimated and unmet medical need:

facts and numbers. J Cachexia Sarcopenia Muscle 1:1-5.

Wahl C, Liptay S, Adler G, Schmid RM (1998). Sulfasalazine: a potent and specific inhibitor of nuclear factor kappa B. J Clin Invest 101:1163-1174.

Whittemore LA, Song K, Li X, Aghajanian J, Davies M, Girgenrath S, Hill JJ, Jalenak M, Kelley P, Knight A, Maylor R, O'Hara D, Pearson A, Quazi A, Ryerson S, Tan XY, Tomkinson KN, Veldman GM, Widom A, Wright JF, Wudyka S, Zhao L, Wolfman NM (2003). Inhibition of myostatin in adult mice increases skeletal muscle mass and strength. Biochem Biophys Res Commun 300:965-971.

Xue H, Sawyer MB, Wischmeyer PE, Baracos VE (2011). Nutrition modulation of gastrointestinal toxicity related to cancer chemotherapy: from preclinical findings to clinical strategy. JPEN J Parenter Enteral Nutr 35:74-90.

Zhou X, Wang JL, Lu J, Song Y, Kwak KS, Jiao Q, Rosenfeld R, Chen Q, Boone T, Simonet WS, Lacey DL, Goldberg AL, Han HQ (2010). Reversal of cancer cachexia and muscle wasting by ActRIIB antagonism leads to prolonged survival. Cell 142:531-543.

FIGURE LEGENDS

Figure 1: Rate of body weight gain of mice from LC cachectic mice (open squares) and those treated with the proteasome (open circles), NF-κB (asterisks), and MAPK (black circles) inhibitors and corresponding control animals (black triangles) over the study period (1 month, N=10/group, all groups). Pharmacological agents were always administered on day 15 after inoculation of the LP07 cells.

Figure 2:

A) Mean values and standard deviation of tyrosine release (nmol/mg/2h) in diaphragm (white bars) and gastrocnemius (black bars) muscles (expressed in Mean values and standard deviation). Statistical significance is represented as follows: i) †††: $p<0.001$ and ††: $p<0.01$ levels in muscles between LC cachectic and control mice and ii) **: $p<0.01$ and *: $p<0.05$ levels in muscles between any group of LC cachectic mice

treated with each of the inhibitors and the LC cachectic animals without any pharmacological treatment (N=10/group, all groups). The dashed line separates both types of comparisons between the groups.

B) Mean values and standard deviation of the ubiquitin conjugating enzyme $E2_{14\kappa}$ in diaphragm (white bars) and gastrocnemius (black bars) muscles, as measured by optical densities in arbitrary units (OD, a.u.). For statistical analysis purposes, the following number of animals was used in each group: control (N=6), LC cachexia (N=8), LC cachexia animals treated with proteasome inhibitor (N=6), LC cachexia mice treated with NF-κB inhibitor (N=8), and LC cachexia rodents treated with MAPK inhibitor (N=8). Statistical significance is represented as follows: i) n.s.: non-significant and †: $p<0.05$ levels in muscles between LC cachectic and control mice and ii) n.s.: non-significant, ***: $p<0.001$, **: $p<0.01$ and *: $p<0.05$ levels in muscles between any group of LC cachectic mice treated with each of the inhibitors and the LC cachectic animals without any pharmacological treatment. The dashed line separates both types of comparisons between the groups.

C) Mean values and standard deviation of 20S proteasome subunit C8 (top panel) and total ubiquitinated proteins (bottom panel) in diaphragm (white bars) and gastrocnemius (black bars) muscles as measured by optical densities in arbitrary units (OD, a.u.). For statistical analysis purposes, the following number of animals was used in each group: control (N=6), LC cachexia (N=8), LC cachexia animals treated with proteasome inhibitor (N=6), LC cachexia mice treated with NF-κB inhibitor (N=8), and LC cachexia rodents treated with MAPK inhibitor (diaphragm, N=7; gastrocnmeius, N=8). Statistical significance is represented as follows: i) n.s.: non-significant, †††: $p<0.001$, and †: $p<0.05$ levels in muscles between LC cachectic and control mice and ii) n.s.: non-significant, ***: $p<0.001$, **: $p<0.01$, and *: $p<0.05$ levels in muscles between any group of LC cachectic mice treated with each of the

31

inhibitors and the LC cachectic animals without any pharmacological treatment. The

dashed line separates both types of comparisons between the groups.

Figure 3:

A) Mean values and standard deviation of NF-κB p50 (top panel) and NF-κB p-p50

(bottom panel) in diaphragm (white bars) and gastrocnemius (black bars) muscles as

measured by optical densities in arbitrary units (OD, a.u.). For statistical analysis

purposes, the following number of animals was used in each group: control (N=6), LC

cachexia (N=8), LC cachexia animals treated with proteasome inhibitor (N=6), LC

cachexia mice treated with NF-κB inhibitor (NF-κB p50, N=8; NF-κB p-p50,

diaphragm N=7; gastrocnemius N=9), and LC cachexia rodents treated with MAPK

inhibitor (NF-κB p50, N=8; NF-κB p-p50, diaphragm N=8; gastrocnemius N=9).

Statistical significance is represented as follows: i) †: p<0.05 levels in muscles

between LC cachectic and control mice and ii) n.s.: non-significant, ***: p<0.001, **:

p<0.01, and *: p<0.05 levels in muscles between any group of LC cachectic mice

treated with each of the inhibitors and the LC cachectic animals without any

pharmacological treatment. The dashed line separates both types of comparisons

between the groups.

B) Mean values and standard deviation of NF-κB p65 (top panel) and NF-κB p-p65

(bottom panel) in diaphragm (white bars) and gastrocnemius (black bars) muscles as

measured by optical densities in arbitrary units (OD, a.u.). For statistical analysis

purposes, the following number of animals was used in each group: control (N=6), LC

cachexia (N=8), LC cachexia animals treated with proteasome inhibitor (N=6), LC

cachexia mice treated with NF-κB inhibitor (N=8), and LC cachexia rodents treated

with MAPK inhibitor (N=8). Statistical significance is represented as follows: i) †:

p<0.05 levels and n.s.: non-significant in muscles between LC cachectic and control

mice and ii) n.s.: non-significant, ***: p<0.001, and *: p<0.05 levels in muscles

32

between any group of LC cachectic mice treated with each of the inhibitors and the LC cachectic animals without any pharmacological treatment. The dashed line separates both types of comparisons between the groups.

C) Mean values and standard deviation IκBα (top panel) and p-IκBα (bottom panel) in diaphragm (white bars) and gastrocnemius (black bars) muscles as measured by optical densities in arbitrary units (OD, a.u.). For statistical analysis purposes, the following number of animals was used in each group: control (N=6), LC cachexia (N=8), LC cachexia animals treated with proteasome inhibitor (N=6), LC cachexia mice treated with NF-κB inhibitor (IκBα, N=8; p-IκBα, diaphragm N=7; gastrocnemius N=8), and LC cachexia rodents treated with MAPK inhibitor (N=8). Statistical significance is represented as follows: i) ††: $p<0.01$ and †: $p<0.05$ levels in muscles between LC cachectic and control mice and ii) ***: $p<0.001$, **: $p<0.01$, *: $p<0.05$, and n.s.: non-significant, levels in muscles between any group of LC cachectic mice treated with each of the inhibitors and the LC cachectic animals without any pharmacological treatment. The dashed line separates both types of comparisons between the groups.

D) Mean values and standard deviation of NF-κB transcriptional activity expressed as the ratio to control gastrocnemius muscles as measured by optical densities in arbitrary units (OD, a.u.). Statistical significance is represented as follows: i) ††: $p<0.01$ levels in muscles between LC cachectic and control mice and ii) *: $p<0.05$ and n.s.: non-significant levels in muscles between any group of LC cachectic mice treated with each of the inhibitors and the LC cachectic animals without any pharmacological treatment (N=10/group, all groups). The dashed line separates both types of comparisons between the groups.

Figure 4:

A) Mean values and standard deviation of myostatin (top panel) and myogenin (bottom

panel) in diaphragm (white bars) and gastrocnemius (black bars) muscles. For statistical analysis purposes, the following number of animals was used in each group: control (N=6), LC cachexia (N=8), LC cachexia animals treated with proteasome inhibitor (N=6), LC cachexia mice treated with NF-κB inhibitor (myostatin, N=9; myogenin, N=8), and LC cachexia rodents treated with MAPK inhibitor (myostatin, N=9; myogenin, diaphragm N=8; gastrocnemius N=7). Statistical significance is represented as follows: i) ††: $p<0.01$ and †: $p<0.05$ levels in muscles between LC cachectic and control mice and ii) ***: $p<0.001$, **: $p<0.01$, *: $p<0.05$, and n.s.: non-significant levels in muscles between any group of LC cachectic mice treated with each of the inhibitors and the LC cachectic animals without any pharmacological treatment. The dashed line separates both types of comparisons between the groups.

B) Mean values and standard deviation of myosin heavy chain (MyHC) (top panel) and actin (bottom panel) levels in diaphragm (white bars) and gastrocnemius (black bars) muscles as measured by optical densities in arbitrary units (OD, a.u.). For statistical analysis purposes, the following number of animals was used in each group: control (MyHC: diaphragm N=7, gastrocnemius N=6; actin N=6), LC cachexia (N=8), LC cachexia animals treated with proteasome inhibitor (N=6), LC cachexia mice treated with NF-κB inhibitor (N=8), and LC cachexia rodents treated with MAPK inhibitor (MyHC: diaphragm N=8, gastrocnemius N=9; actin, N=8). Statistical significance is represented as follows: i) ††: $p<0.01$ and †: $p<0.05$ levels in muscles between LC cachectic and control mice and ii) ***: $p<0.001$, *: $p<0.05$, and n.s.: non-significant levels in muscles between any group of LC cachectic mice treated with each of the inhibitors and the LC cachectic animals without any pharmacological treatment. The dashed line separates both types of comparisons between the groups.

Figure 5: Mean values and standard deviation of the autophagy protein LC3-II/LC3-I in diaphragm (white bars) and gastrocnemius (black bars) muscles as measured by optical

densities in arbitrary units (OD, a.u.). For statistical analysis purposes, the following number of animals was used in each group: control (N=6), LC cachexia (N=8), LC cachexia animals treated with proteasome inhibitor (N=6), LC cachexia mice treated with NF-κB inhibitor (diaphragm, N=8; gastrocnemius, N=9), and LC cachexia rodents treated with MAPK inhibitor (diaphragm, N=8; gastrocnemius, N=9). Statistical significance is represented as follows: i) †: p<0.05 levels in muscles between LC cachectic and control mice and ii) **: p<0.01, *: p<0.05, and n.s.: non-significant levels in muscles between any group of LC cachectic mice treated with each of the inhibitors and the LC cachectic animals without any pharmacological treatment. The dashed line separates both types of comparisons between the groups.

Figure 6:

A) Representative examples obtained from the diaphragm muscle of the different study groups of animals. Myofibers positively stained with the anti-MyHC type II antibody are stained in brown color (x 400). Type I fibers are represented in white color (not stained).

B) Representative examples obtained from the gastrocnemius muscle of the different study groups of animals. Myofibers positively stained with the anti-MyHC type II antibody are stained in brown color (x 400). Type I fibers are represented in white color (not stained).

C) Representative examples of nuclei positively (arrows) and negatively stained for the TUNEL assay in the diaphragm muscles of the different study groups of mice (x 400). Negative nuclei appear in blue (hematoxylin counterstaining), while TUNEL-positive nuclei are brown.

D) Representative examples of nuclei positively (arrows) and negatively stained for the TUNEL assay in the gastrocnemius muscles of the different study groups of mice (x 400). Negative nuclei appear in blue (hematoxylin counterstaining), while TUNEL-

35

positive nuclei are brown.

Table 1. Physiological characteristics in mice from all groups at the end of the study period (day 30)

				Lung cancer cachexia					
	Control	LC cachexia	p	Proteasome inhibitor	p	NF-κβ inhibitor	p	MAPK inhibitor	p
Body weight gain (%)	+8.97 (2.72)	-7.69 (12.89)	†††	-11.72 (8.14)	n.s.	+0.42 (7.26)	**	-0.30 (5.59)	**
Diaphragm weight (g)	0.089 (0.009)	0.067 (0.012)	†††	0.071 (0.01)	n.s.	0.08 (0.007)	***	0.076 (0.009)	*
Gastrocnemius weight (g)	0.114 (0.008)	0.087 (0.016)	†††	0.086 (0.009)	n.s.	0.101 (0.01)	***	0.094 (0.009)	*
Limb strength gain (%)	+10.27 (19.59)	-11.7 (15.37)	†††	-12.2 (24.04)	n.s.	+3.04 (12.9)	**	+0.49 (9.27)	***
Sc. Tumor weight (g)	-	1.42 (0.59)	-	1.17 (0.56)	*	1.03 (0.31)	**	0.57 (0.32)	***

Variables are presented as mean (SD).

Definition of abbreviations: LC, Lung Cancer; NF-κB, Nuclear Factor-κB; MAPK, Mitogen-activated protein kinases; Sc., subcutaneous.

Statistical significance: †††, p≤0.001 between LC cachectic and control mice; n.s., non-significant,* p≤0.05, **, p≤0.01 and ***, p≤0.001 between any of the treated mouse groups with cachexia and LC cachexia only animals. Grey shades have been used to highlight the significant comparisons between the different groups.

Table 2. Structural and cellular markers in respiratory and limb muscles of all study groups of animals

					Lung cancer cachexia					
	Muscle	Control	LC cachexia	p	Proteasome inhibitor	p	NF-κB inhibitor	p	MAPK inhibitor	p
					Fiber type composition					
Type I fibers (%)	Diaphragm	9.04 (2.05)	8.22 (2.61)	n.s.	8.59 (1.37)	n.s.	8.12 (1.02)	n.s.	6.64 (1.89)	n.s.
	Gastrocnemius	13.4 (2.74)	13.17 (2.61)	n.s.	11.94 (2.97)	n.s.	14.3 (2.35)	n.s.	14.5 (2.97)	n.s.
Type II fibers (%)	Diaphragm	90.96 (2.05)	91.78 (2.61)	n.s.	91.41 (1.37)	n.s.	91.98 (1.02)	n.s.	93.4 (1.89)	n.s.
	Gastrocnemius	86.6 (2.74)	86.83 (2.98)	n.s.	88.06 (2.97)	n.s.	85.7 (2.35)	n.s.	85.5 (2.97)	n.s.
Type I fibers area (µm^2)	Diaphragm	326.1 (66.59)	233.4 (33.54)	††	320.8 (66)	**	237 (83.71)	n.s.	280 (28.9)	**
	Gastrocnemius	951.7 (109.7)	658.8 (122.6)	†††	824.6 (88.7)	**	754.7 (98.8)	n.s.	792.5 (102)	*
Type II fibers area (µm^2)	Diaphragm	382.5 (82.7)	297.1 (68)	†	319.9 (66.5)	n.s.	297.1 (68)	n.s.	291 (35.3)	n.s.
	Gastrocnemius	919.2 (135.1)	723.5 (143.9)	†	764 (93.8)	n.s.	742.9 (121.5)	n.s.	793 (91.3)	n.s.
					Muscle abnormalities					
Abnormal fraction (%)	Diaphragm	8.16 (1.43)	14.61 (3.75)	†††	11.97 (3.16)	n.s.	11.56 (3.9)	n.s.	13.1 (2.81)	n.s.
	Gastrocnemius	3.93 (1.48)	8.15 (1.8)	†††	8.39 (2.18)	n.s.	7.05 (1.3)	n.s.	4.93 (1.21)	***
Inflamatory cells (%)	Diaphragm	3.75 (0.62)	6.51 (1.54)	†††	5.18 (1.03)	*	4.67 (1.78)	*	4.66 (1.1)	**
	Gastrocnemius	2.22 (0.99)	5.45 (1.78)	†††	4.91 (1.14)	n.s.	3.52 (0.63)	**	2.78 (0.88)	***
Internal nuclei (%)	Diaphragm	4.01 (1.44)	7.18 (3.5)	†	6.38 (2.79)	n.s.	6.11 (1.9)	n.s.	7.88 (1.47)	n.s.
	Gastrocnemius	1.59 (0.68)	2.36 (0.8)	†	3.28 (0.98)	*	3.25 (1.07)	*	2.08 (0.69)	n.s.
TUNEL-stained nuclei (%)	Diaphragm	46.08 (8.55)	67.85 (10.62)	†††	60.9 (17.93)	n.s.	64.1 (11.86)	n.s.	60.2 (6.57)	*
	Gastrocnemius	49.71 (12.93)	69.88 (12.62)	†††	70.77 (9.74)	n.s.	64.09 (10.4)	n.s.	70.7 (9.47)	n.s.

Variables are presented as mean (SD).

Definition of abbreviations: LC, Lung Cancer; NF-κB, Nuclear Factor-κB; MAPK, Mitogen-activated protein kinases; µm;

micrometer.

Statistical significance: n.s., non-significant, †, p≤0.05, ††≤0.01 and †††, p≤0.001 between LC cachectic and control mice; n.s., non-significant, * p≤0.05, **, p≤0.01 and ***, p≤0.001 between any of the treated mouse groups with cachexia and LC cachexia only animals.

Grey shades have been used to highlight the significant comparisons between the different groups.
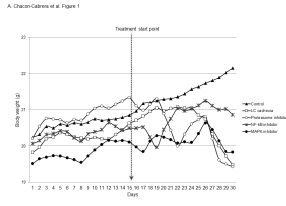
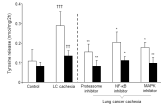Figure1 .

A. Chacon-Cabrera et al. Figure 2A
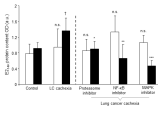

Figure2A .

A. Chacon-Cabrera et al. Figure 2B

Figure2B .
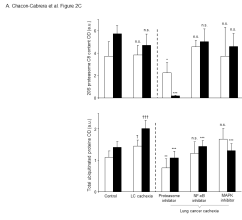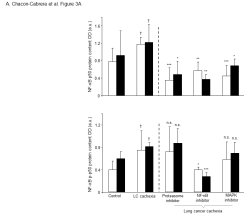
Figure2C .

Figure3A .
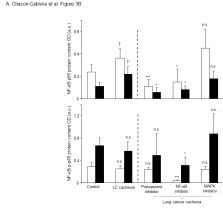
Figure3B .

A. Chacon-Cabrera et al. Figure 3C
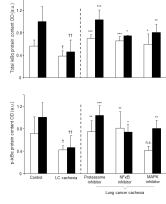
Figure3C .

A. Chacon-Cabrera et al. Figure 3D
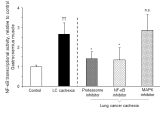
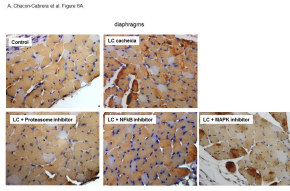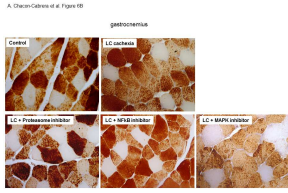Figure3D .
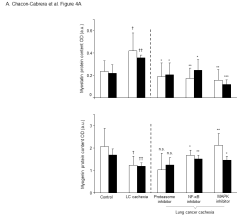
Figure4A .
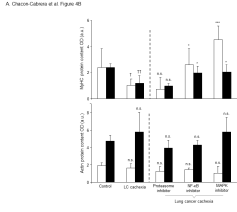
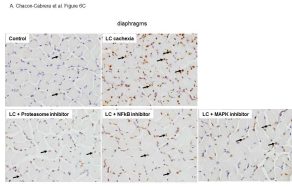Figure4B .

A. Checcon-Cabrera et al. Figure 5
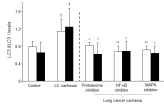
Figure5 .

Figure6A .

Figure6B .

Figure6C .

Figure6D .